

DF-3DFace: One-to-Many Speech Synchronized 3D Face Animation with Diffusion

Se Jin Park, Joanna Hong, Minsu Kim, Yong Man Ro*

Image and Video Systems Lab, KAIST
{jinny960812, joanna2587, ms.k, ymro}@kaist.ac.kr

Abstract

Speech-driven 3D facial animation has gained significant attention for its ability to create realistic and expressive facial animations in 3D space based on speech. Learning-based methods have shown promising progress in achieving accurate facial motion synchronized with speech. However, one-to-many nature of speech-to-3D facial synthesis has not been fully explored: while the lip accurately synchronizes with the speech content, other facial attributes beyond speech-related motions are variable with respect to the speech. To account for the potential variance in the facial attributes within a single speech, we propose DF-3DFace, a diffusion-driven speech-to-3D face mesh synthesis. DF-3DFace captures the complex one-to-many relationships between speech and 3D face based on diffusion. It concurrently achieves aligned lip motion by exploiting audio-mesh synchronization and masked conditioning. Furthermore, the proposed method jointly models identity and pose in addition to facial motions so that it can generate 3D face animation without requiring a reference identity mesh and produce natural head poses. We contribute a new large-scale 3D facial mesh dataset, 3D-HDTF to enable the synthesis of variations in identities, poses, and facial motions of 3D face mesh. Extensive experiments demonstrate that our method successfully generates highly variable facial shapes and motions from speech and simultaneously achieves more realistic facial animation than the state-of-the-art methods.

1. Introduction

Speech-driven 3D facial animation aims to generate facial movements that accurately reflect the corresponding speech sounds with natural and realistic facial motion. It has been gaining increasing attention for its ability to represent vivid facial movements in 3D space and its applicability to the animation industries, *e.g.*, 3D games, and virtual reality, where the avatars animate in a 3D environment.

Among the works in speech-driven 3D facial animation, learning-based methods (Fan et al. 2022a; Cudeiro et al. 2019; Xing et al. 2023; Richard et al. 2021b; Cao et al. 2005; Fan et al. 2022b; Habibie et al. 2021; Pham, Wang, and Pavlovic 2018; Wang, Fan, and Xia 2021; Taylor et al. 2017; Karras et al. 2017) have recently shown significant progress in achieving realistic facial motion in sync with speech. They adopt a data-driven approach, utilizing paired audio-mesh

data to generate facial animation for a given speaker in a 3D vertex space. These methods employ techniques such as latent space learning (Richard et al. 2021b; Xing et al. 2023), audio feature extraction (Cudeiro et al. 2019), and transformer model (Fan et al. 2022a) and direct toward improving the accuracy of facial motion for resolving the highly ill-posed audio-visual mapping task.

Despite numerous efforts to generate accurate 3D facial motion from speech, the one-to-many nature of speech-to-facial synthesis has not been well addressed. Input speech can decide mouth movements and rough facial shape, but it cannot precisely determine facial attributes that have weak correlations with the speech (Xing et al. 2023; Tang et al. 2022; Ma et al. 2023). To be specific, the same person can speak the same utterance with variations in speaking style, movement of the eyebrows, eyelids, and head pose. Yet, current works deterministically synthesize 3D face animation from speech through one-to-one mapping. Furthermore, the synthesis is mostly restricted to the inner facial motion (Fan et al. 2022a; Xing et al. 2023; Karras et al. 2017; Fan et al. 2022b; Wang, Fan, and Xia 2021; Richard et al. 2021b). To elaborate, the identity component of the 3D face from the speech is not synthesized but is given at the input as an identity template mesh which is the mesh of the reference identity in neutral expression. Also, the head pose is left for manual control. 3D face datasets are mostly in neutral head pose. Existing 3D face datasets with synchronized audio (Fanelli et al. 2010a; Karras et al. 2017; Cudeiro et al. 2019; Richard et al. 2021a; Wu et al. 2022) are limited because they are shot in a controlled environment with static poses or static expressions and contain only dozens of characters with a few minutes of utterance. Such limited scope of 3D face datasets presents a constraint in capturing diverse and natural 3D facial animations.

To tackle the aforementioned challenge, we propose DF-3DFace, a novel framework for speech-to-3D face synthesis. DF-3DFace employs a diffusion mechanism to capture the complex one-to-many relationships between speech and 3D face mesh, introducing stochasticity to the animation. It generates diverse facial animations while maintaining high-fidelity lip motion by exploiting mesh-audio synchronization and masked conditioning. We model identity and head pose in addition to facial motion to achieve more comprehensive facial animations. We show that the three facial components

*Corresponding author.

can not only be generated directly from speech but also be individually controlled by providing the reference at the input. Since existing 3D face datasets (Fanelli et al. 2010a; Karras et al. 2017; Cudeiro et al. 2019; Richard et al. 2021a; Wu et al. 2022) lack diversity in the facial motions and shapes, we construct a new large-scale 3D facial mesh dataset, namely 3D-HDTF, from a large-scale high-resolution 2D talking face dataset (Zhang et al. 2021). Leveraging the 3D-HDTF, we build a scalable and unified 3D face animation model that captures variations in identities, poses, and facial motions of 3D face mesh from speech.

Our contributions are four-fold: (1) We propose one-to-many speech synchronized DF-3DFace, a novel speech-to-3D face mesh generation framework based on diffusion. Our diffusion approach enables diverse 3D facial animation from a single speech while fulfilling lip synchronization. (2) We model identity, head pose, and facial motion to achieve comprehensive 3D facial animation driven by speech. Each component can also be independently adjusted, providing controllability to the diverse generation. (3) We construct a large-scale 3D facial mesh dataset namely 3D-HDTF from a 2D talking face video dataset (HDTF) (Zhang et al. 2021) using a 3D face reconstruction technique (Feng et al. 2021). The 3D-HDTF facilitates the learning of diverse and natural variations of identities, poses, and facial motions. (4) Through extensive experiments, we demonstrate that DF-3DFace successfully captures the one-to-many relationships between speech and 3D face mesh, while achieving superior lip synchronization and realism compared to state-of-the-art methods.

2. Related Works

2.1. Speech-driven 3D Facial Animation

Speech-driven 3D facial animation uses speech signals to generate realistic and expressive 3D facial movements in 3D vertex space. Previous works on speech-driven 3D facial animation have focused on learning the accurate mapping between audio and face mesh in terms of facial motion (Cao et al. 2005; Taylor et al. 2017; Zhou et al. 2018; Karras et al. 2017; Cudeiro et al. 2019; Richard et al. 2021b; Fan et al. 2022a; Xing et al. 2023; Zhou et al. 2018). For example, (Cao et al. 2005) employs Anime Graph structure and a search-based mechanism. (Taylor et al. 2017) takes a sliding window approach and a re-targeting technique to animate unseen identities. VOCA (Cudeiro et al. 2019) utilizes subject conditioning to capture individual speaking styles. Meshtalk (Richard et al. 2021b) disentangles audio-correlated and -uncorrelated information in a categorical latent space, and autoregressively samples an audio-conditioned temporal model. Faceformer (Fan et al. 2022a) encodes long-term audio context based on transformer (Vaswani et al. 2017) to achieve temporally stable and accurate lip synchronization. CodeTalker (Xing et al. 2023) utilizes a codebook with discrete primitives (Van Den Oord, Vinyals et al. 2017) to reduce the audio-visual mapping uncertainty. Although prior works can synthesize high-fidelity face mesh from speech, they only enable deterministic one-to-one mapping between the speech-to-face mesh. Moreover, they require an identity template mesh as an input to precisely synthesize corresponding facial motions.

In this paper, we formulate the task as one-to-many and aim to capture variations in facial motion and jointly synthesize identity and head pose from speech.

2.2. 3D Face Dataset

3D face dataset (Zhu et al. 2021; Paysan et al. 2009; Cao et al. 2013; Savran et al. 2008; Yin et al. 2006; Zhang et al. 2016, 2014, 2013; Fanelli et al. 2010b; Alashkar et al. 2014) is a collection of 3D scans of human faces capturing dynamic facial expressions and poses for applications such as facial recognition, animation, and expression analysis. Yet, only a few datasets (Cudeiro et al. 2019; Fanelli et al. 2010a; Cudeiro et al. 2019; Karras et al. 2017; Zhang and Fisher 2019; Richard et al. 2021a) provide synchronized audio, and they are critically scale-limited. First, they do not support a wide range of identities and phonemes. BIWI (Fanelli et al. 2010a) and VOCASET (Cudeiro et al. 2019) are common benchmarks but BIWI (Fanelli et al. 2010a) records only 40 sentences for each of 14 subjects while VOCASET records 255 sentences from 12 subjects. S3DFM (Zhang and Fisher 2019) contains 100 subjects with only one unique utterance for each subject. Multiface (Wuu et al. 2022) records 36 hours of utterance from 250 subjects but a small fraction of the dataset, comprising 13 subjects speaking 50 sentences, has been made publicly available. Additionally, the recordings are captured in a controlled environment at a studio, with subjects either in static poses or with static expressions. On the other hand, large-scale 2D talking face datasets (Afouras et al. 2018; Afouras, Chung, and Zisserman 2018; Chung, Nagrani, and Zisserman 2018; Chung and Zisserman 2017; Nagrani, Chung, and Zisserman 2017; Wang et al. 2020; Zhang et al. 2021) are readily accessible and have allowed for the rapid development of speech-driven 2D talking face generation (Park et al. 2022; Zhou et al. 2021; Prajwal et al. 2020; Wang et al. 2021; Guo et al. 2021; Hong et al. 2022; Liang et al. 2022; Zhou et al. 2019; Wu et al. 2021). To this end, we transform one of the large-scale 2D talking face datasets, HDTF (Zhang et al. 2021) into a 3D face mesh dataset, namely 3D-HDTF. While the reconstructed 3D faces may not match the fidelity of actual 3D scans, they not only capture a wide variety of facial shapes and motions but also natural head pose and expression while talking. Leveraging the 3D-HDTF, we build a scalable and generalizable speech-driven 3D face animation model.

2.3. Diffusion Generation

Diffusion model is a generative model based on the stochastic diffusion process to generate samples from a probability distribution (Sohl-Dickstein et al. 2015; Ho, Jain, and Abbeel 2020). It starts with a Gaussian noise distribution and iteratively applies a sequence of diffusion steps. Each diffusion step adds Gaussian noise with increasing variance, and the reverse diffusion step removes the Gaussian noise from the sample to get a sample from the target distribution. By iteratively sampling the data distribution starting from the initial noise, it can transform the noise into a complex distribution that resembles the target distribution. With its powerful capability of generating diverse and high-fidelity samples, it has greatly succeeded in image synthesis (Dhariwal and

Nichol 2021; Song, Meng, and Ermon 2020; Ramesh et al. 2022; Saharia et al. 2022; Rombach et al. 2022; Nichol et al. 2021). Recently, the diffusion model has been applied to talking face generation (Stypulkowski et al. 2023; Shen et al. 2023; Du et al. 2023) which synthesizes 2D face video conditioned on speech. However, they diffuse at the pixel level to generate high-fidelity images without considering the temporality of the facial motion. Our work is more aligned with motion diffusion models (Zhang et al. 2022; Ma, Bai, and Zhou 2022; Tevet et al. 2022) which synthesize human body motion conditioned on textual description. In this paper, we aim to synthesize 3D face mesh conditioned on speech. We take the first approach to employ diffusion to enable precise and one-to-many mapping between speech and face mesh in terms of identity, pose, and motion.

3. Method

An overview of our method is illustrated in Figure 1. We extract identity representation $\mathbf{x}_{\text{id}} \in \mathbb{R}^{3V}$, facial motion representation $\mathbf{x}_{\text{motion}} \in \mathbb{R}^{N \times 3V}$, and head pose representation $\mathbf{x}_{\text{pose}} \in \mathbb{R}^{N \times 3}$ from a 3D face mesh sequence $\mathbf{v} \in \mathbb{R}^{N \times 3V}$ of length N and channel size of V vertices. The aim is to learn the joint data distribution of the three representations conditioned on input audio \mathbf{a} , $p(\mathbf{X}|\mathbf{a})$ where $\mathbf{X} = [\mathbf{x}_{\text{id}}, \mathbf{x}_{\text{motion}}, \mathbf{x}_{\text{pose}}]$ is denoted as the face representations. We introduce 3D face mesh diffusion model which jointly diffuses the face representations and enables one-to-many 3D face animation while aligning the lip motion with the input speech. At inference, the face representations are sampled from the learned data distribution, where each component of the face representations can be individually controlled.

3.1. 3D Face Mesh Representations

To synthesize identity and pose along with facial motion, we disentangle a 3D face mesh sequence $\mathbf{v} \in \mathbb{R}^{N \times 3V}$ into identity representation \mathbf{x}_{id} , pose representation \mathbf{x}_{pose} , and facial motion representation $\mathbf{x}_{\text{motion}}$. In this section, we explain how we have factored out each of the components in 3D mesh space so that the face mesh can be re-rendered without losing information.

Identity Representation Identity contains facial features and structures that are unique to each individual. To eliminate the variance of the mesh due to the change in head pose, we first transform the face mesh sequence \mathbf{v} into zero head pose by applying the Linear blend skinning (LBS) (Loper et al. 2015). By forcing the global pose vector of the reconstructed pose parameter θ to zero, the face mesh sequence \mathbf{v} is transformed into zero pitch, roll, and yaw. We take the average of randomly sampled K zero pose face meshes $\mathbf{x}_{\text{zeropose}}$ for individual subjects as the identity representation, $\mathbf{x}_{\text{id}} = \frac{1}{K} \sum_i^K \mathbf{x}_{\text{zeropose}}^i$.

Pose Representation Pose refers to the orientation of the face in 3D space. From the 3D face reconstruction method (Feng et al. 2021), we obtain the pose parameter θ for each timestep t , from which we extract the global rotation vector, $\mathbf{x}_{\text{pose}} = \{\theta_{\text{global}}^t\}_{t=1}^N$.

Motion Representation Facial motion, which we shorten as motion, includes dynamics of the inner face including facial expressions reflecting emotion, movement of the mouth and jaw in sync with speech, eyebrow raising, and eye blinking. To capture such dynamics, we represent the motion as the deviation of the vertices in the zero pose face mesh $\mathbf{x}_{\text{zeropose}}^t$ from the corresponding identity representation \mathbf{x}_{id} as $\mathbf{x}_{\text{motion}} = \{\mathbf{x}_{\text{zeropose}}^t - \mathbf{x}_{\text{id}}\}_{t=1}^N$.

3.2. 3D Face Mesh Diffusion

To enable one-to-many mapping from speech \mathbf{a} to the face representations $\mathbf{X} = [\mathbf{x}_{\text{id}}, \mathbf{x}_{\text{motion}}, \mathbf{x}_{\text{pose}}]$ as obtained in section 3.1, we model the data distribution $p(\mathbf{X}|\mathbf{a})$ based on diffusion (Ho, Jain, and Abbeel 2020).

The diffusion defines a forward noising process $q(x_t|x_{t-1})$, for $t \in [0, T]$ as a Gaussian distribution following a Markov chain,

$$q(x_t|x_{t-1}) = \mathcal{N}(\sqrt{\alpha_t}x_{t-1}, (1 - \alpha_t)I), \quad (1)$$

where clean sample x_0 is repeatedly corrupted into pure noise $x_T = \mathcal{N}(0, I)$ controlled by a predefined variance scheduler α_t . The denoising step, which is the reverse of the noising step, is also defined as a Gaussian distribution,

$$p(x_{t-1}|x_t) = \mathcal{N}(\mu_\theta(x_t, t), \sigma_\theta(x_t, t)I), \quad (2)$$

where the pure noise x_T is iteratively denoised back to a clean sample x_0 based on the mean $\mu_\theta(\cdot)$ and variance $\sigma_\theta(\cdot)$ parameterized using a deep neural network.

In our context, we model audio-conditioned face representation $p(\mathbf{X}|\mathbf{a})$ with the reverse diffusion process of predicting clean face representation \mathbf{X}_0 from noised face representations \mathbf{X}_t conditioned on audio \mathbf{a} (x_0 – formulation (Ramesh et al. 2022)). During training, we uniformly sample $t \in [0, T]$ and obtain noised face representation \mathbf{X}_t at diffusion timestep t from $q(\mathbf{X}_t|\mathbf{X}_0) = \mathcal{N}(\sqrt{\bar{\alpha}_t}\mathbf{X}_0, (1 - \bar{\alpha}_t)I)$ where $\bar{\alpha}_t = \prod_{s=1}^t \alpha_s$. Given the diffusion step t , audio \mathbf{a} , and diffused face representation \mathbf{X}_t , we implement a diffusion model G_θ , based on transformer-encoder (Vaswani et al. 2017), to predict the clean face representation $\hat{\mathbf{X}}_0$ as follows,

$$\hat{\mathbf{X}}_0 = G_\theta(t, \mathbf{a}, \mathbf{X}_t). \quad (3)$$

The audio representation $\mathbf{a} \in \mathbb{R}^{N_a \times Z_a}$ is extracted using the state-of-the-art ASR model, Hu-BERT (Hsu et al. 2021). The face representation $\mathbf{X} \in \mathbb{R}^{(N+1) \times (3V+3)}$ is formulated as a concatenation of the motion representation $\mathbf{x}_{\text{motion}} \in \mathbb{R}^{N \times 3V}$ and pose representation $\mathbf{x}_{\text{pose}} \in \mathbb{R}^{N \times 3}$ along channel axis, denoted as the motion pose representation $\mathbf{x}_{\text{MP}} \in \mathbb{R}^{N \times (3V+3)}$, followed by a concatenation of the identity representation $\mathbf{x}_{\text{id}} \in \mathbb{R}^{3V}$ along the time axis (with additional zero-padded 3 dimension). For each frame in the diffused face representation \mathbf{X}_t , we individually project identity, motion, and pose representations to match the diffusion latent space \mathbb{R}^C . The diffusion timestep t and audio representation \mathbf{a} are also individually projected and \mathbf{a} is resampled to match the length of the mesh sequence N . The projected audio representation and face representation are summed with their respective modality embeddings and positional embeddings. Then, they

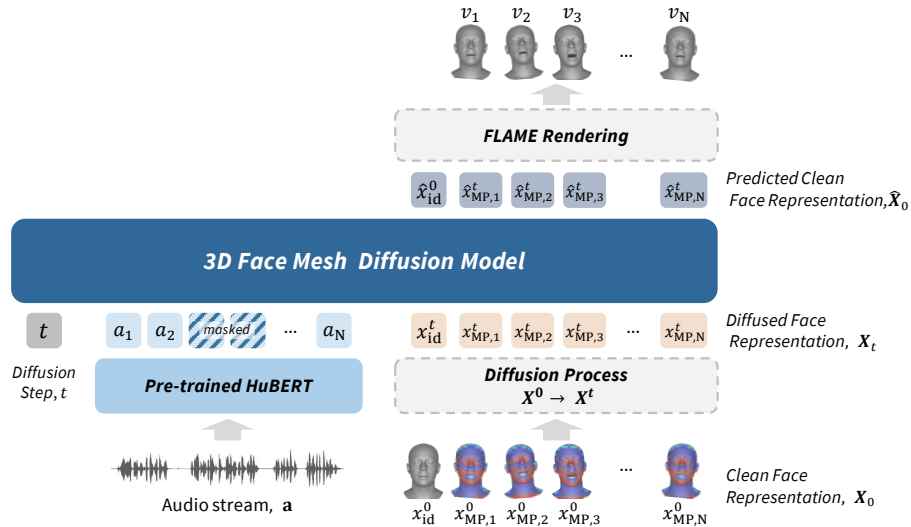


Figure 1: Overview of our DF-3DFace framework. The clean face representation $\mathbf{X}_0 = [x_{\text{id}}^0, x_{\text{MP}, 1:N}^0]$ is noised into \mathbf{X}_t through the diffusion process. Given the diffusion timestep t , randomly masked HuBERT audio representation \mathbf{a} , and diffused face representation \mathbf{X}_t , 3D face mesh diffusion model learns to predict clean face representation $\hat{\mathbf{X}}_0$. The predicted clean face representation $\hat{\mathbf{X}}_0$ is then rendered as a sequence of 3D face mesh. Note that the motion pose representations $x_{\text{MP}, 1:N}$ are visualized as heat maps where regions with higher values are in the color red while the lower are in the color blue.

are concatenated along the time axis with the projected diffusion timestep t as the first token, forming the input tokens $\mathbb{R}^{(2N+2) \times C}$. From the output, we exclude the first $(N+1)$ output tokens (corresponding to t and \mathbf{a}) and project the rest back to the original mesh space to obtain the predicted clean face representations $\hat{\mathbf{X}}_0 \in \mathbb{R}^{(N+1) \times (3V+3)}$.

We employ the standard denoising diffusion loss,

$$\mathcal{L}_{\text{face}} = \mathbb{E}_{(\mathbf{X}_0, \mathbf{a}), t \sim [1, T]} [\|\mathbf{X}_0 - G_\theta(t, \mathbf{a}, \mathbf{X}_t)\|_2^2]. \quad (4)$$

3.3. Masked Conditioning

We introduce masked conditioning $\mathcal{M}_{\text{cond}}$ to improve diversity while minimizing trade-offs in the fidelity of lip synchronization. In practice, classifier-free guidance (Ho and Salimans 2022) learns both conditioned and unconditioned distributions by randomly setting the condition $c = \emptyset$ for 10% of the samples during training and sampling the interpolation of the two variants during inference. It has been used in tasks that have more freedom in generation such as class-conditioned and text-conditioned image generation (Saharia et al. 2022; Nichol et al. 2021; Dhariwal and Nichol 2021), video generation (Ho et al. 2022a,b) and human body motion generation (Zhang et al. 2023; Ma, Bai, and Zhou 2022). However, our task is more tightly bound by the condition as the mesh has to timely align with the audio. Simply setting the audio to null would hurt the lip sync performance. Thus, we apply random mask m to 10% of the audio representations \mathbf{a} during training and interpolate between the masked conditioned and unmasked conditioned distributions with the hyperparameter s during inference as follows,

$$G_\theta(t, \mathbf{a}, \mathbf{X}_t) = G_\theta(t, m(\mathbf{a}), \mathbf{X}_t) \quad (5)$$

$$+ s \cdot (G_\theta(t, \mathbf{a}, \mathbf{X}_t) - G_\theta(t, m(\mathbf{a}), \mathbf{X}_t)). \quad (6)$$

3.4. Mesh and Audio Synchronization

To accurately synchronize the 3D face mesh with the audio, we propose a 3D mesh-based sync expert. We train a sync expert $\mathcal{S}_{\text{sync}}$ such that it measures the likelihood that the input audio and the 3D face mesh is in-sync, inspired by (Prajwal et al. 2020). Specifically, we randomly select segments of face representation $x_{\text{motion}}^{i:i+n}$ of length n and apply a lip mask m_{lip} which selects vertices pertaining to the mouth region in the motion representation x_{motion} . The sync expert calculates the cosine similarity distance between the mouth motion and audio representations $a^{i:i+n}$ which is extracted from HuBERT (Hsu et al. 2021). The sync expert is trained to minimize the distance between synchronized pairs while maximizing the distance between out-of-sync pairs. More training details can be found in the supplementary. The trained sync expert is then fixed and used to guide the DF-3DFace to enhance speech-lip synchronization of the synthesized facial motions $\hat{x}_{\text{motion}}^{i:i+n}$ with the following sync loss $\mathcal{L}_{\text{sync}}$,

$$\mathcal{L}_{\text{sync}} = \mathbb{E}_{(\hat{x}_{\text{motion}}, \mathbf{a}), i \sim [1, N-n]} [\mathcal{S}_{\text{sync}}(m_{\text{lip}} \cdot \hat{x}_{\text{motion}}^{i:i+n}, a^{i:i+n})]. \quad (7)$$

3.5. Auxiliary Loss

To place greater emphasis on the mouth and pose, which constitute the majority of the dynamics in the mesh, we additionally apply lip loss \mathcal{L}_{lip} , and pose loss $\mathcal{L}_{\text{pose}}$ as follows,

$$\mathcal{L}_{\text{lip}} = \mathbb{E}_{\hat{x}_{\text{motion}}} [\|m_{\text{lip}} \cdot (\mathbf{x}_{\text{motion}} - \hat{x}_{\text{motion}})\|_2^2], \quad (8)$$

$$\mathcal{L}_{\text{pose}} = \mathbb{E}_{\hat{x}_{\text{pose}}, i \sim [1, N-1]} [\|(x_{\text{pose}}^{i+1} - x_{\text{pose}}^i) - (\hat{x}_{\text{pose}}^{i+1} - \hat{x}_{\text{pose}}^i)\|_2^2]. \quad (9)$$

The lip loss \mathcal{L}_{lip} measures the MSE loss between the predicted and ground facial motion (\hat{x}_{motion} and x_{motion} respectively)

Method	Dataset	Avg Lip Vertex Error↓ ($\times 10^{-5}$ mm)	Max Lip Vertex Error↓ ($\times 10^{-5}$ mm)	Non-Lip Deviation↓ ($\times 10^{-4}$ mm)
MeshTalk (Richard et al. 2021b)	VOCASET	2.734	6.910	1.818
Faceformer (Fan et al. 2022a)	VOCASET	2.655	7.521	1.790
CodeTalker (Xing et al. 2023)	VOCASET	2.492	6.406	1.749
DF-3DFace	VOCASET	2.489	6.545	2.253
MeshTalk (Richard et al. 2021b)	3D-HDTF*	0.646	1.567	3.295
Faceformer (Fan et al. 2022a)	3D-HDTF*	0.510	1.214	2.823
CodeTalker (Xing et al. 2023)	3D-HDTF*	2.679	5.617	4.449
DF-3DFace	3D-HDTF*	0.430	1.037	0.970
DF-3DFace w/o \mathbf{x}_{id}	3D-HDTF	0.421	1.029	0.635
DF-3DFace w/o \mathbf{x}_{pose}	3D-HDTF	0.423	1.045	0.644
DF-3DFace w/o \mathcal{L}_{lip}	3D-HDTF	0.434	1.041	0.648
DF-3DFace w/o \mathcal{L}_{sync}	3D-HDTF	0.452	1.073	0.647
DF-3DFace w/o \mathcal{L}_{pose}	3D-HDTF	0.430	1.038	0.650
DF-3DFace w/o \mathcal{M}_{cond}	3D-HDTF	0.433	1.037	0.636
DF-3DFace	3D-HDTF	0.496	1.204	0.776

Table 1: Quantitative evaluation on VOCASET, 3D-HDTF*, and 3D-HDTF.

of the mouth region using the lip mask m_{lip} . As the movement of the pose is more dynamic than the facial motion, the pose transition needs to be smooth so we apply a pose loss \mathcal{L}_{pose} which brings the difference of adjacent pose representations of the ground truth mesh close to that of the generated mesh. Note that we have dropped the notation for the diffusion timestep of 0. The losses are scaled with respective hyperparameters λ and summed to give the final training loss,

$$\mathcal{L} = \lambda_{face}\mathcal{L}_{face} + \lambda_{sync}\mathcal{L}_{sync} + \lambda_{lip}\mathcal{L}_{lip} + \lambda_{pose}\mathcal{L}_{pose}. \quad (10)$$

3.6. Sampling

Starting from a Gaussian noise $\mathbf{X}_T \sim \mathcal{N}(0, I)$, we iteratively sample $\mathbf{X}_{t-1} \sim p_{\theta}(\mathbf{X}_{t-1}|\mathbf{X}_t, \mathbf{a})$ until the final clean face representation $\hat{\mathbf{X}}_0$ is reached. $p_{\theta}(\mathbf{X}_{t-1}|\mathbf{X}_t, \mathbf{a})$ follows a Gaussian distribution $\mathcal{N}(\mu_{\theta}, \sigma I)$, where $\mu_{\theta} = \sqrt{\bar{\alpha}_{t-1}}G_{\theta}(t, \mathbf{a}, \mathbf{X}_t)$ and $\sigma = (1 - \bar{\alpha}_{t-1})I$ are the mean and variance, induced from the predicted clean face representation $\hat{\mathbf{X}}_0 = G_{\theta}(t, \mathbf{a}, \mathbf{X}_t)$ at diffusion timestep t . Starting from the pure noise and iteratively sampling from the predicted Gaussian distributions leads to multiple different facial animations across multiple sampling processes. Although the face representation as a whole is jointly diffused, we enable individual control of the identity, pose, and motion during sampling. Specifically, instead of generating all three representations given an audio input \mathbf{a} , we can give any combinations of the identity, pose, and motion as target references. For example, to generate a mesh of a reference identity speaking the input audio, we input the target reference identity instead of sampling from the Gaussian noise, and at each iteration during sampling, we overwrite the identity representations of the output with its target reference. Therefore, DF-3DFace can not only synthesize diverse identities, pose, and motions from a single speech but also synthesize with the given reference. This is in contrast to the existing approach where the scheme is limited to animating the given identity in static head pose.

3.7. Mesh Rendering

Once we obtain the face representation $\mathbf{X} = [\mathbf{x}_{id}, \mathbf{x}_{motion}, \mathbf{x}_{pose}] \in \mathbb{R}^{(N+1) \times (3V+3)}$ from the diffu-

sion model G_{θ} , we render it back to the original face mesh $\mathbf{v} \in \mathbb{R}^{N \times 3V}$ by reversing the steps in section 3.1. We first add identity representation \mathbf{x}_{id} to each of the motion representation \mathbf{x}_{motion} to get zero pose face mesh $\mathbf{x}_{zeropose}$. Then we deform the zero pose face mesh $\mathbf{x}_{zeropose}$ with the pose representation \mathbf{x}_{pose} based on LBS (Loper et al. 2015).

4. Experiments

4.1. Datasets

3D-HDTF Since existing 3D face databases are critically limited in size and scope to hold a natural and diverse range of 3D faces while talking, we construct a 3D-HDTF. 3D-HDTF is synthesized from a large in-the-wild high-resolution talking face audio-visual dataset (HDTF) (Zhang et al. 2021). It contains 300 speakers with 15.8 hours of approximately 10,000 utterances, captured at 30 fps and collected from youtube. We use the 3D face reconstruction method (Feng et al. 2021) to obtain mesh in FLAME topology as has been applied in (Cudeiro et al. 2019; Feng et al. 2021; Sanyal et al. 2019; Ghosh et al. 2020; Cao et al. 2005; Ranjan et al. 2018). Please refer to the supplementary for the implementation detail of the reconstruction model.

3D-HDTF* We additionally introduce a zero-pose version of the 3D-HDTF namely 3D-HDTF* to fairly compare with the prior works that can not synthesize the head pose. Each mesh is transformed into zero head pose position using the linear blend skinning (Loper et al. 2015).

VOCASET VOCASET (Cudeiro et al. 2019) is a popular 3D face scan dataset. It has 12 speakers with 480 3D facial motion sequences captured at 60fps with a duration of 3 to 4 seconds each. There are 255 unique sentences, some of which are shared between the speakers. We use the train, validation, and test splits provided by VOCASET.

4.2. Evaluation Metrics

Lip Synchronization We follow the evaluation protocol employed in state-of-the-works (Cudeiro et al. 2019; Richard et al. 2021b; Fan et al. 2022a; Xing et al. 2023) to measure

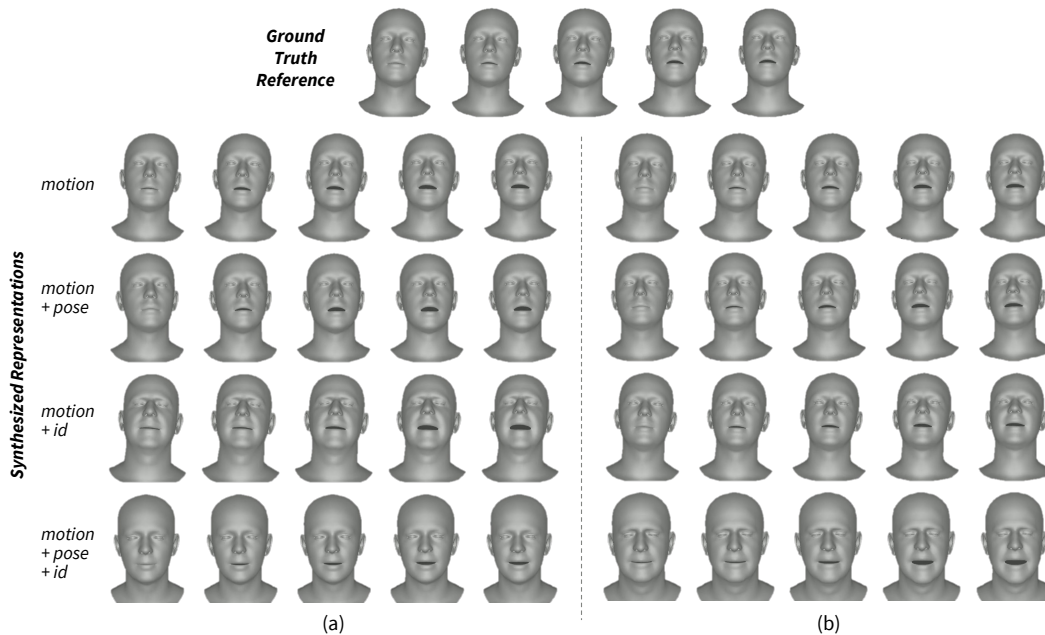


Figure 2: Generation results by DF-3DFace where different components of the face representations have been synthesized as indicated on the left, and sampling has been performed twice in (a) and (b). While consistently achieving accurate lip synchronization, DF-3DFace generates diverse 3D face animations with controllable identity, motion, and pose. We encourage readers to zoom in for details.

Comparison	VOCASET		3D-HDTF*		3D-HDTF	
	Realism	Lip Sync	Realism	Lip Sync	Realism	Lip Sync
DF-3DFace vs GT	40.28 ± 3.66	57.78 ± 4.20	50.72 ± 1.93	51.71 ± 2.13	65.56 ± 2.45	69.39 ± 1.99
DF-3DFace vs MeshTalk	70.56 ± 1.87	68.89 ± 1.97	72.58 ± 1.92	73.29 ± 1.63	–	–
DF-3DFace vs Facformer	48.56 ± 2.96	51.11 ± 2.13	60.47 ± 2.92	62.39 ± 2.29	–	–
DF-3DFace vs CodeTalker	49.17 ± 2.18	50.89 ± 2.21	63.69 ± 1.89	64.10 ± 1.88	–	–

Table 2: User study on VOCASET, 3D-HDTF*, and 3D-HDTF. The score indicates preference of DF-3DFace over others in %

lip synchronization. The lip synchronization is measured with lip-vertex error which is the maximal L2 distance of lip vertices between the prediction and the ground truth.

Non-Lip Dynamics Deviation We implement non-lip dynamics deviation (NLDD) motivated by (Xing et al. 2023) to evaluate the dynamics of the non-lip part of the face mesh. It computes the difference in the standard deviation of element-wise L2 norm along the temporal axis between the predicted and ground truth non-lip vertices.

Multimodality We evaluate the variability of the generation by calculating how much the generation diversifies within each given audio as proposed in (Guo et al. 2020). Given an input audio, it generates two subsets with the same sample size of 100 and calculates the L2 distance between the two subsets. We measure the multimodality in terms of mesh v , identity x_{id} , motion x_{motion} , and pose x_{pose} .

4.3. Quantitative Evaluation

Lip Synchronization & Non-lip Deviation We quantitatively compare our DF-3DFace with state-of-the-art methods, Meshtalk (Richard et al. 2021b), Faceformer (Fan et al.

2022a), and Codetalker (Xing et al. 2023) in Table 1. Implementation details of DF-3DFace and the comparison methods are provided in the supplementary. Since these methods only synthesize facial motion given the identity and audio, we evaluate the facial motion on the zero-pose datasets (VOCASET and 3D-HDTF*). On both datasets, DF-3DFace achieves lower lip vertex error, producing more synchronized lip movement than the state-of-the-art methods. As our method jointly synthesizes the identity, the non-lip deviation is apparently higher on VOCASET which contains minimal variance in the non-lip region. But it achieves significantly superior performance on the 3D-HDTF* which encompasses more variations in the facial shapes and motions. The result demonstrates the effectiveness of our method in generating a wide range of 3D face meshes from speech.

Variability & Controllability We validate the variability and controllability in Table 3. DF-3DFace introduces stochasticity through the diffusion process and enables one-to-many mapping as demonstrated by the multimodality scores. This is in contrast to prior works that learn the deterministic one-to-one mapping between speech and mesh. We also measure the

Method	Input	Output	Mult _{id} [↑] ($\times 10^{-6}$ mm)	Mult _{motion} [↑] ($\times 10^{-7}$ mm)	Mult _{pose} [↑] ($\times 10^{-3}$ mm)	Mult _{mesh} [↑] ($\times 10^{-6}$ mm)
DF-3DFace	aud, id, pose	motion	0.000	1.813	0.000	0.197
	aud, pose	motion, id	1.834	1.916	0.000	2.091
	aud, id	motion, pose	0.000	1.813	2.910	80.779
	aud	motion, pose, id	1.834	1.916	5.212	152.130
+ w/o $\mathcal{M}_{\text{cond}}$	aud	motion, pose, id	0.313	0.660	1.311	31.601

Table 3: Multimodality Evaluation on 3D-HDTF.

multimodality of each component of the face representations when provided with different references at the input. The result indicates that giving identity as a reference constrains the variance of the motion and pose while giving pose as a reference does not affect the variance of the motion and identity. This is because the range of possible motion and pose can be narrowed down with the specified identity. The mesh multimodality is the highest when only audio is given and decreases as more references are incorporated. Also, the result verifies independent controllability of the identity, motion, and pose because those provided as the references have zero multimodality, allowing variance only in the non-referenced components.

4.4. Qualitative Evaluation

We refer to the demo video for detailed qualitative evaluation as the sync quality and naturalness are best viewed over time with the audio. Compared with the baseline methods, our method not only generates the most synchronized lip movements but also captures the natural and diverse range of facial motions present in the 3D-HDTF* dataset. On the 3D-HDTF*, Faceformer and Meshtalk portray motions confined to the lip region only, which makes the animation unrealistic. CodeTalker captures the motions across the face including the eyeblinks but sometimes the face is deformed arbitrarily. In contrast, our method portrays the dynamics over the entire face most similar to the ground truth, based on the diffusion process which accurately models the complex relationship between speech and 3D face mesh from the dataset.

Generation results in Figure 2 further illustrate variability and controllability of identity, pose, and motion. We synthesize with different references from the ground truth, and sample twice in Figure 2 (a) and (b). The second row is when identity and pose are provided as references and only motion is synthesized. The pose and identity align with the ground truth reference while there is variance only in motion where (a) and (b) have different eye blinks. When the pose is synthesized in the third row, it exhibits variations in the pose where a) is posing right upward and (b) straight upward. When identity is synthesized, there are subtle variations in the shape of the skull and the size of the jawline as shown in the last two rows. While capturing variations in facial attributes from a single speech and allowing controllability, DF-3DFace achieves synchronized lip. Please refer to the demo video and supplementary for detailed demonstrations.

User Study We conduct A/B tests for perceptual evaluation in Table 2. We asked 20 participants to choose the better sample in terms of realism and lip synchronization when

presented with side-by-side clips of our approach versus others. We randomly select 15 to 20 samples for each dataset, giving a total of 180 clips. Note that we only evaluate the 3D-HDTF against the ground truth because other methods do not support pose synthesis. Our method surpasses lip synchronization, and the performance gap is even larger when synthesizing more dynamic animation in 3D-HDTF. Interestingly, our method even outperforms the ground truth, indicating that it models the data distribution with high-fidelity lip synchronization based on the mesh-audio synchronization learning, compensating for the reconstruction error that occurred during the data construction.

4.5. Ablation Study

Identity and Pose Representations Please note that the following ablations in Table 1 are conducted without masked conditioning $\mathcal{M}_{\text{cond}}$. Without learning x_{id} or x_{pose} , lip synchronization and non-lip deviation both improve as the model can focus on learning the facial motion. Yet, it enables synthesis and manipulation over identity and pose with negligible performance overhead.

Loss Functions Both lip loss \mathcal{L}_{lip} and sync loss $\mathcal{L}_{\text{sync}}$ contribute to lip synchronization and the effect of the sync loss is greater than the lip loss. The pose loss $\mathcal{L}_{\text{pose}}$ improves non-lip deviation with a trade-off between lip synchronization. The three losses altogether give the best performance.

Masked Conditioning Masked conditioning effectively boosts diversity where mesh multimodality $\text{Mult}_{\text{mesh}}$ increases by nearly 5 times as shown in Table 3 with a tradeoff in the lip vertex error as shown in Table 1. Note that the experiments were performed with $s = 1$. Please refer to the supplementary for comprehensive experiments of the diversity hyperparameter s and % of masking.

5. Conclusion

We present DF-3DFace, a novel framework for one-to-many speech-synchronized 3D facial animation. It enables variations of the 3D face from a single speech while ensuring lip synchronization by exploiting audio-mesh synchronization and masked conditioning. Our diffusion-based approach effectively captures the natural and diverse range of 3D faces present in the constructed 3D-HDTF. Also, DF-3DFace models the identity, pose, and motion for a comprehensive animation and additionally allows controllability to each component. Through extensive experiments, we validate the effectiveness of the proposed DF-3DFace in incorporating diversity and achieving high-fidelity 3D facial animation.

References

- Afouras, T.; Chung, J. S.; Senior, A.; Vinyals, O.; and Zisserman, A. 2018. Deep audio-visual speech recognition. *IEEE transactions on pattern analysis and machine intelligence*, 44(12): 8717–8727.
- Afouras, T.; Chung, J. S.; and Zisserman, A. 2018. LRS3-TED: a large-scale dataset for visual speech recognition. *arXiv preprint arXiv:1809.00496*.
- Alashkar, T.; Amor, B. B.; Daoudi, M.; and Berretti, S. 2014. A 3D dynamic database for unconstrained face recognition. In *5th International Conference and Exhibition on 3D Body Scanning Technologies*.
- Cao, C.; Weng, Y.; Zhou, S.; Tong, Y.; and Zhou, K. 2013. Facewarehouse: A 3d facial expression database for visual computing. *IEEE Transactions on Visualization and Computer Graphics*, 20(3): 413–425.
- Cao, Y.; Tien, W. C.; Faloutsos, P.; and Pighin, F. 2005. Expressive speech-driven facial animation. *ACM Transactions on Graphics (TOG)*, 24(4): 1283–1302.
- Chung, J. S.; Nagrani, A.; and Zisserman, A. 2018. Voxceleb2: Deep speaker recognition. *arXiv preprint arXiv:1806.05622*.
- Chung, J. S.; and Zisserman, A. 2017. Lip reading in the wild. In *Computer Vision-ACCV 2016: 13th Asian Conference on Computer Vision, Taipei, Taiwan, November 20-24, 2016, Revised Selected Papers, Part II 13*, 87–103. Springer.
- Cudeiro, D.; Bolkart, T.; Laidlaw, C.; Ranjan, A.; and Black, M. J. 2019. Capture, learning, and synthesis of 3D speaking styles. In *Proceedings of the IEEE/CVF Conference on Computer Vision and Pattern Recognition*, 10101–10111.
- Dhariwal, P.; and Nichol, A. 2021. Diffusion models beat gans on image synthesis. *Advances in Neural Information Processing Systems*, 34: 8780–8794.
- Du, C.; Chen, Q.; He, T.; Tan, X.; Chen, X.; Yu, K.; Zhao, S.; and Bian, J. 2023. DAE-Talker: High Fidelity Speech-Driven Talking Face Generation with Diffusion Autoencoder. *arXiv preprint arXiv:2303.17550*.
- Fan, Y.; Lin, Z.; Saito, J.; Wang, W.; and Komura, T. 2022a. Faceformer: Speech-driven 3d facial animation with transformers. In *Proceedings of the IEEE/CVF Conference on Computer Vision and Pattern Recognition*, 18770–18780.
- Fan, Y.; Lin, Z.; Saito, J.; Wang, W.; and Komura, T. 2022b. Joint audio-text model for expressive speech-driven 3d facial animation. *Proceedings of the ACM on Computer Graphics and Interactive Techniques*, 5(1): 1–15.
- Fanelli, G.; Gall, J.; Romsdorfer, H.; Weise, T.; and Gool, L. V. 2010a. A 3-D Audio-Visual Corpus of Affective Communication. *IEEE Transactions on Multimedia*, 12(6): 591–598.
- Fanelli, G.; Gall, J.; Romsdorfer, H.; Weise, T.; and Van Gool, L. 2010b. A 3-d audio-visual corpus of affective communication. *IEEE Transactions on Multimedia*, 12(6): 591–598.
- Feng, Y.; Feng, H.; Black, M. J.; and Bolkart, T. 2021. Learning an Animatable Detailed 3D Face Model from In-The-Wild Images. volume 40.
- Ghosh, P.; Gupta, P. S.; Uziel, R.; Ranjan, A.; Black, M. J.; and Bolkart, T. 2020. GIF: Generative interpretable faces. In *2020 International Conference on 3D Vision (3DV)*, 868–878. IEEE.
- Guo, C.; Zuo, X.; Wang, S.; Zou, S.; Sun, Q.; Deng, A.; Gong, M.; and Cheng, L. 2020. Action2motion: Conditioned generation of 3d human motions. In *Proceedings of the 28th ACM International Conference on Multimedia*, 2021–2029.
- Guo, Y.; Chen, K.; Liang, S.; Liu, Y.-J.; Bao, H.; and Zhang, J. 2021. Ad-nerf: Audio driven neural radiance fields for talking head synthesis. In *Proceedings of the IEEE/CVF International Conference on Computer Vision*, 5784–5794.
- Habibie, I.; Xu, W.; Mehta, D.; Liu, L.; Seidel, H.-P.; Pons-Moll, G.; Elgharib, M.; and Theobalt, C. 2021. Learning speech-driven 3d conversational gestures from video. In *Proceedings of the 21st ACM International Conference on Intelligent Virtual Agents*, 101–108.
- Ho, J.; Chan, W.; Saharia, C.; Whang, J.; Gao, R.; Gritsenko, A.; Kingma, D. P.; Poole, B.; Norouzi, M.; Fleet, D. J.; et al. 2022a. Imagen video: High definition video generation with diffusion models. *arXiv preprint arXiv:2210.02303*.
- Ho, J.; Jain, A.; and Abbeel, P. 2020. Denoising diffusion probabilistic models. *Advances in Neural Information Processing Systems*, 33: 6840–6851.
- Ho, J.; and Salimans, T. 2022. Classifier-free diffusion guidance. *arXiv preprint arXiv:2207.12598*.
- Ho, J.; Salimans, T.; Gritsenko, A.; Chan, W.; Norouzi, M.; and Fleet, D. J. 2022b. Video diffusion models. *arXiv preprint arXiv:2204.03458*.
- Hong, F.-T.; Zhang, L.; Shen, L.; and Xu, D. 2022. Depth-aware generative adversarial network for talking head video generation. In *Proceedings of the IEEE/CVF Conference on Computer Vision and Pattern Recognition*, 3397–3406.
- Hsu, W.-N.; Bolte, B.; Tsai, Y.-H. H.; Lakhotia, K.; Salakhutdinov, R.; and Mohamed, A. 2021. Hubert: Self-supervised speech representation learning by masked prediction of hidden units. *IEEE/ACM Transactions on Audio, Speech, and Language Processing*, 29: 3451–3460.
- Karras, T.; Aila, T.; Laine, S.; Herva, A.; and Lehtinen, J. 2017. Audio-driven facial animation by joint end-to-end learning of pose and emotion. *ACM Transactions on Graphics (TOG)*, 36(4): 1–12.
- Liang, B.; Pan, Y.; Guo, Z.; Zhou, H.; Hong, Z.; Han, X.; Han, J.; Liu, J.; Ding, E.; and Wang, J. 2022. Expressive talking head generation with granular audio-visual control. In *Proceedings of the IEEE/CVF Conference on Computer Vision and Pattern Recognition*, 3387–3396.
- Loper, M.; Mahmood, N.; Romero, J.; Pons-Moll, G.; and Black, M. J. 2015. SMPL: A skinned multi-person linear model. *ACM transactions on graphics (TOG)*, 34(6): 1–16.
- Ma, J.; Bai, S.; and Zhou, C. 2022. Pretrained Diffusion Models for Unified Human Motion Synthesis. *arXiv preprint arXiv:2212.02837*.
- Ma, Y.; Wang, S.; Hu, Z.; Fan, C.; Lv, T.; Ding, Y.; Deng, Z.; and Yu, X. 2023. StyleTalk: One-shot Talking Head Generation with Controllable Speaking Styles. *arXiv preprint arXiv:2301.01081*.

- Nagrani, A.; Chung, J. S.; and Zisserman, A. 2017. Voxceleb: a large-scale speaker identification dataset. *arXiv preprint arXiv:1706.08612*.
- Nichol, A.; Dhariwal, P.; Ramesh, A.; Shyam, P.; Mishkin, P.; McGrew, B.; Sutskever, I.; and Chen, M. 2021. Glide: Towards photorealistic image generation and editing with text-guided diffusion models. *arXiv preprint arXiv:2112.10741*.
- Park, S. J.; Kim, M.; Hong, J.; Choi, J.; and Ro, Y. M. 2022. Synctalkface: Talking face generation with precise lip-syncing via audio-lip memory. In *Proceedings of the AAAI Conference on Artificial Intelligence*, volume 36, 2062–2070.
- Paysan, P.; Knothe, R.; Amberg, B.; Romdhani, S.; and Vetter, T. 2009. A 3D face model for pose and illumination invariant face recognition. In *2009 sixth IEEE international conference on advanced video and signal based surveillance*, 296–301. Ieee.
- Pham, H. X.; Wang, Y.; and Pavlovic, V. 2018. End-to-end learning for 3d facial animation from speech. In *Proceedings of the 20th ACM International Conference on Multimodal Interaction*, 361–365.
- Prajwal, K.; Mukhopadhyay, R.; Namboodiri, V. P.; and Jawahar, C. 2020. A lip sync expert is all you need for speech to lip generation in the wild. In *Proceedings of the 28th ACM International Conference on Multimedia*, 484–492.
- Ramesh, A.; Dhariwal, P.; Nichol, A.; Chu, C.; and Chen, M. 2022. Hierarchical text-conditional image generation with clip latents. *arXiv preprint arXiv:2204.06125*.
- Ranjan, A.; Bolkart, T.; Sanyal, S.; and Black, M. J. 2018. Generating 3D faces using convolutional mesh autoencoders. In *Proceedings of the European conference on computer vision (ECCV)*, 704–720.
- Richard, A.; Lea, C.; Ma, S.; Gall, J.; De la Torre, F.; and Sheikh, Y. 2021a. Audio-and gaze-driven facial animation of codec avatars. In *Proceedings of the IEEE/CVF winter conference on applications of computer vision*, 41–50.
- Richard, A.; Zollhöfer, M.; Wen, Y.; De la Torre, F.; and Sheikh, Y. 2021b. Meshtalk: 3d face animation from speech using cross-modality disentanglement. In *Proceedings of the IEEE/CVF International Conference on Computer Vision*, 1173–1182.
- Rombach, R.; Blattmann, A.; Lorenz, D.; Esser, P.; and Ommer, B. 2022. High-resolution image synthesis with latent diffusion models. In *Proceedings of the IEEE/CVF Conference on Computer Vision and Pattern Recognition*, 10684–10695.
- Saharia, C.; Chan, W.; Saxena, S.; Li, L.; Whang, J.; Denton, E. L.; Ghasemipour, K.; Gontijo Lopes, R.; Karagol Ayan, B.; Salimans, T.; et al. 2022. Photorealistic text-to-image diffusion models with deep language understanding. *Advances in Neural Information Processing Systems*, 35: 36479–36494.
- Sanyal, S.; Bolkart, T.; Feng, H.; and Black, M. J. 2019. Learning to regress 3D face shape and expression from an image without 3D supervision. In *Proceedings of the IEEE/CVF Conference on Computer Vision and Pattern Recognition*, 7763–7772.
- Savran, A.; Alyüz, N.; Dibeklioglu, H.; Çeliktutan, O.; Gökerberk, B.; Sankur, B.; and Akarun, L. 2008. Bosphorus database for 3D face analysis. In *Biometrics and Identity Management: First European Workshop, BIOID 2008, Roskilde, Denmark, May 7-9, 2008. Revised Selected Papers 1*, 47–56. Springer.
- Shen, S.; Zhao, W.; Meng, Z.; Li, W.; Zhu, Z.; Zhou, J.; and Lu, J. 2023. DiffTalk: Crafting Diffusion Models for Generalized Talking Head Synthesis. *arXiv preprint arXiv:2301.03786*.
- Sohl-Dickstein, J.; Weiss, E.; Maheswaranathan, N.; and Ganguli, S. 2015. Deep unsupervised learning using nonequilibrium thermodynamics. In *International Conference on Machine Learning*, 2256–2265. PMLR.
- Song, J.; Meng, C.; and Ermon, S. 2020. Denoising diffusion implicit models. *arXiv preprint arXiv:2010.02502*.
- Stypułkowski, M.; Vougioukas, K.; He, S.; Zięba, M.; Petridis, S.; and Pantic, M. 2023. Diffused Heads: Diffusion Models Beat GANs on Talking-Face Generation. *arXiv preprint arXiv:2301.03396*.
- Tang, A.; He, T.; Tan, X.; Ling, J.; Li, R.; Zhao, S.; Song, L.; and Bian, J. 2022. Memories are One-to-Many Mapping Alleviators in Talking Face Generation. *arXiv preprint arXiv:2212.05005*.
- Taylor, S.; Kim, T.; Yue, Y.; Mahler, M.; Krahe, J.; Rodriguez, A. G.; Hodgins, J.; and Matthews, I. 2017. A deep learning approach for generalized speech animation. *ACM Transactions On Graphics (TOG)*, 36(4): 1–11.
- Tevet, G.; Raab, S.; Gordon, B.; Shafir, Y.; Cohen-Or, D.; and Bermano, A. H. 2022. Human motion diffusion model. *arXiv preprint arXiv:2209.14916*.
- Van Den Oord, A.; Vinyals, O.; et al. 2017. Neural discrete representation learning. *Advances in neural information processing systems*, 30.
- Vaswani, A.; Shazeer, N.; Parmar, N.; Uszkoreit, J.; Jones, L.; Gomez, A. N.; Kaiser, Ł.; and Polosukhin, I. 2017. Attention is all you need. *Advances in neural information processing systems*, 30.
- Wang, K.; Wu, Q.; Song, L.; Yang, Z.; Wu, W.; Qian, C.; He, R.; Qiao, Y.; and Loy, C. C. 2020. Mead: A large-scale audio-visual dataset for emotional talking-face generation. In *Computer Vision—ECCV 2020: 16th European Conference, Glasgow, UK, August 23–28, 2020, Proceedings, Part XXI*, 700–717. Springer.
- Wang, Q.; Fan, Z.; and Xia, S. 2021. 3d-talkemo: Learning to synthesize 3d emotional talking head. *arXiv preprint arXiv:2104.12051*.
- Wang, S.; Li, L.; Ding, Y.; Fan, C.; and Yu, X. 2021. Audio2head: Audio-driven one-shot talking-head generation with natural head motion. *arXiv preprint arXiv:2107.09293*.
- Wu, H.; Jia, J.; Wang, H.; Dou, Y.; Duan, C.; and Deng, Q. 2021. Imitating arbitrary talking style for realistic audio-driven talking face synthesis. In *Proceedings of the 29th ACM International Conference on Multimedia*, 1478–1486.
- Wuu, C.-h.; Zheng, N.; Ardisson, S.; Bali, R.; Belko, D.; Brockmeyer, E.; Evans, L.; Godisart, T.; Ha, H.; Hypes,

- A.; Koska, T.; Krenn, S.; Lombardi, S.; Luo, X.; McPhail, K.; Millerschoen, L.; Perdoch, M.; Pitts, M.; Richard, A.; Saragih, J.; Saragih, J.; Shiratori, T.; Simon, T.; Stewart, M.; Trimble, A.; Weng, X.; Whitewolf, D.; Wu, C.; Yu, S.-I.; and Sheikh, Y. 2022. Multiface: A Dataset for Neural Face Rendering. In *arXiv*.
- Xing, J.; Xia, M.; Zhang, Y.; Cun, X.; Wang, J.; and Wong, T.-T. 2023. CodeTalker: Speech-Driven 3D Facial Animation with Discrete Motion Prior. In *Proceedings of the IEEE/CVF Conference on Computer Vision and Pattern Recognition (CVPR)*.
- Yin, L.; Wei, X.; Sun, Y.; Wang, J.; and Rosato, M. J. 2006. A 3D facial expression database for facial behavior research. In *7th international conference on automatic face and gesture recognition (FGR06)*, 211–216. IEEE.
- Zhang, J.; and Fisher, R. B. 2019. 3d visual passcode: Speech-driven 3d facial dynamics for biometrics. *Signal processing*, 160: 164–177.
- Zhang, M.; Cai, Z.; Pan, L.; Hong, F.; Guo, X.; Yang, L.; and Liu, Z. 2022. Motiondiffuse: Text-driven human motion generation with diffusion model. *arXiv preprint arXiv:2208.15001*.
- Zhang, M.; Guo, X.; Pan, L.; Cai, Z.; Hong, F.; Li, H.; Yang, L.; and Liu, Z. 2023. ReMoDiffuse: Retrieval-Augmented Motion Diffusion Model. *arXiv preprint arXiv:2304.01116*.
- Zhang, X.; Yin, L.; Cohn, J. F.; Canavan, S.; Reale, M.; Horowitz, A.; and Liu, P. 2013. A high-resolution spontaneous 3d dynamic facial expression database. In *2013 10th IEEE international conference and workshops on automatic face and gesture recognition (FG)*, 1–6. IEEE.
- Zhang, X.; Yin, L.; Cohn, J. F.; Canavan, S.; Reale, M.; Horowitz, A.; Liu, P.; and Girard, J. M. 2014. Bp4d-spontaneous: a high-resolution spontaneous 3d dynamic facial expression database. *Image and Vision Computing*, 32(10): 692–706.
- Zhang, Z.; Girard, J. M.; Wu, Y.; Zhang, X.; Liu, P.; Ciftci, U.; Canavan, S.; Reale, M.; Horowitz, A.; Yang, H.; et al. 2016. Multimodal spontaneous emotion corpus for human behavior analysis. In *Proceedings of the IEEE conference on computer vision and pattern recognition*, 3438–3446.
- Zhang, Z.; Li, L.; Ding, Y.; and Fan, C. 2021. Flow-guided one-shot talking face generation with a high-resolution audio-visual dataset. In *Proceedings of the IEEE/CVF Conference on Computer Vision and Pattern Recognition*, 3661–3670.
- Zhou, H.; Liu, Y.; Liu, Z.; Luo, P.; and Wang, X. 2019. Talking face generation by adversarially disentangled audio-visual representation. In *Proceedings of the AAAI conference on artificial intelligence*, volume 33, 9299–9306.
- Zhou, H.; Sun, Y.; Wu, W.; Loy, C. C.; Wang, X.; and Liu, Z. 2021. Pose-controllable talking face generation by implicitly modularized audio-visual representation. In *Proceedings of the IEEE/CVF conference on computer vision and pattern recognition*, 4176–4186.
- Zhou, Y.; Xu, Z.; Landreth, C.; Kalogerakis, E.; Maji, S.; and Singh, K. 2018. Visemenet: Audio-driven animator-centric speech animation. *ACM Transactions on Graphics (TOG)*, 37(4): 1–10.
- Zhu, H.; Yang, H.; Guo, L.; Zhang, Y.; Wang, Y.; Huang, M.; Shen, Q.; Yang, R.; and Cao, X. 2021. FacesCape: 3D facial dataset and benchmark for single-view 3D face reconstruction. *arXiv preprint arXiv:2111.01082*.